Approaching the Zero-Outage Capacity of MIMO-OFDM Without Instantaneous Water-Filling

Joon Hyun Sung and John R. Barry, *Senior Member, IEEE*

***Abstract*—Orthogonal-frequency-division multiplexing (OFDM) transforms a frequency-selective multiple-input multiple-output (MIMO) fading channel into a MIMO-OFDM channel that has a well-defined outage capacity. A transmitter with channel knowledge can achieve this capacity by a combination of *eigenbeamforming* and *water-filling*; the eigenbeamforming transforms the MIMO-OFDM channel into a parallel bank of scalar channels, and the water-filling procedure optimally allocates rate and energy to the scalar channels—a form of adaptive modulation. This paper shows that the water-filling procedure is not necessary to approach the zero-outage capacity of the MIMO-OFDM channel; it is sufficient instead to use a combination of eigenbeamforming and a fixed (nonadaptive) rate allocation. The fixed allocation depends only on the statistics of the channel and is independent of the particular channel realization. This paper proves that the capacity penalty incurred by the fixed allocation approaches zero as the number of antennas grows large. Numerical results indicate that the convergence is fast; for example, the fixed allocation suffers an SNR penalty of less than 0.2 dB for a 6-input 6-output Rayleigh-fading MIMO-OFDM channel at 8 bits per signaling interval, when the channel is assumed to be uncorrelated between antennas and between channel taps. A main conclusion is that eigenbeamforming is the most valuable way to exploit knowledge of the channel at the transmitter, and that any subsequent adaptive modulation has minimal relative value.**

***Index Terms*—Closed-loop multiple-input-multiple-output orthogonal-frequency-division multiplexing, eigenbeamforming, fading channels, outage capacity, rate allocation.**

I. Introduction

INFORMATION theory for single-user communications over fading channels has been thoroughly studied for decades [1]. Two types of capacity measures have emerged: the *average* or ergodic capacity, and the *outage* capacity. The availability of channel-state information (CSI) at the transmitter does not dramatically impact the *average* capacity of a single-input–single-output (SISO) channel [2]. The same is true for a multiple-input–multiple-output (MIMO) channel at high signal-to-noise ratio (SNR) [3]–[6]. On the other hand, transmitter CSI has a dramatic impact on the *outage* capacity of both SISO [7] and MIMO [8] channels.

This paper concerns the outage capacity. In particular, we use the *zero-outage* capacity, also known as the delay-limited capacity [1], [9], as a metric for the maximum achievable rate of fading channels with a zero outage probability. When outages are unavoidable, the zero-outage capacity is zero. A positive zero-outage capacity can be achieved only when the transmitter knows CSI [1], but even this is not always enough; for example, the zero-outage capacity is zero with transmitter CSI on a Rayleigh flat-fading SISO channel [2]. However, when there is *diversity* [10], such as from frequency selectivity or from multiple antennas, a positive zero-outage capacity can be achieved with the knowledge of CSI at the transmitter [1], [7], [11]. Not surprisingly, MIMO channels can have a large zero-outage capacity due to the spatial diversity from its antenna arrays at both ends. In fact, on a Rayleigh-flat-fading channel, the zero-outage capacity is not only nonzero, but also approaches the *average* capacity as the number of antennas tends to infinity [8].

We consider the *MIMO-OFDM channel*, which is the effective channel that results from an application of orthogonal-frequency-division multiplexing (OFDM) to a frequency-selective fading MIMO channel, and which has a well-defined outage capacity. We assume that the underlying frequency-selective channel is uncorrelated between channel taps. A transmitter with CSI can achieve this capacity by a combination of *eigenbeamforming* [12] and *water-filling*; the eigenbeamforming transforms the MIMO-OFDM channel into a parallel bank of scalar channels, and the water-filling procedure optimally allocates rate and energy to the scalar channels, a classical *power-allocation* problem in information theory [13].

In this paper, we show that the zero-outage capacity can be approached with one of two simpler allocations: the *frequency-uniform-spectral-efficiency (FUSE)* allocation or the *fixed-rate (FIXED)* allocation. The FUSE allocation forces each OFDM tone to have the same spectral efficiency, so that the problem of water-filling jointly over space and frequency reduces to a set of independent water-fillings over space only, once for each OFDM tone. The FIXED allocation is totally nonadaptive, with no water-filling at all; instead, the rates are deterministically allocated to match the channel statistics, independent of the particular channel realization. We will see that, despite their reduced complexity, the FUSE and FIXED allocations are nearly optimal in terms of the zero-outage capacity they achieve. The main contributions of this paper are as follows:

- we introduce the FUSE and FIXED allocation strategies, and we derive their optimal allocation (Proposition 1 and Proposition 3);

Manuscript received May 25, 2007; revised November 15, 2007. This research was supported in part by National Science Foundation Grants CCR-0082329 and CCR-0121565, and by the Yamacraw program.

J. H. Sung is with Samsung Advanced Institute of Technology, Seoul, South Korea 158-730 (e-mail: joonhyun.sung@samsung.com).

J. R. Barry is with the Department of Electrical and Computer Engineering, Georgia Institute of Technology, Atlanta, GA 30332 USA (e-mail: barry@ece.gatech.edu).

Communicated by A. J. Goldsmith, Associate Editor for Communications.

Color versions of Figures 2–7 in this paper are available online at http://ieeexplore.ieee.org.

Digital Object Identifier 10.1109/TIT.2008.917698

- we prove that the penalties of the FUSE and FIXED allocations, relative to the optimal water-filling over space and frequency, converge to zero when the number of antenna tends to infinity (Proposition 2 and Proposition 4);
- we present high-SNR analysis which shows that the penalties of the FUSE and FIXED allocations are small for a moderate number of antennas (Proposition 5 and Proposition 6).

The analytic results for the FUSE and FIXED allocations can immediately apply to a practical closed-loop MIMO-OFDM system, providing theoretical limits and potentials for practical allocation strategies [14], [15].

The rest of paper is organized as follows. Section II describes a model for the MIMO fading frequency-selective channel, and it reviews how a frequency-selective MIMO channel is converted into a bank of scalar channels by OFDM and eigenbeamforming. Section III introduces the power-allocation problem and proposes the FUSE and FIXED allocations. We also analyze the limiting performance of the FUSE and FIXED allocations as the number of antennas goes to infinity. In Section IV, we conduct high-SNR analysis to show that the penalties of the FUSE and FIXED allocations quickly converge to zero. Section V provides numerical results via Monte Carlo simulations. Finally we conclude in Section VI.

II. System Model

We consider the following linear discrete-time baseband MIMO channel with M_T transmit and M_R receive antennas:

$$\boldsymbol{y}_k = \sum_{l=0}^{L} \mathbf{G}_l \boldsymbol{x}_{k-l} + \boldsymbol{n}_k \tag{1}$$

where $\boldsymbol{x}_k$ is the $M_T \times 1$ vector of symbols transmitted during the kth signaling interval, and $\boldsymbol{y}_k$ is the $M_R \times 1$ vector of received samples for the kth signaling interval, and where $\mathbf{G}_l$ is the $M_R \times M_T$ channel matrix for the l-th delay. The channel memory is denoted by L, so that the channel is flat-fading (memoryless) when $L = 0$, and it can be frequency-selective when $L > 0$. We assume that realizations of $\{\mathbf{G}_l\}$ are randomly chosen at the beginning of transmission and remain fixed for all channel uses [5]. The $M_R \times 1$ noise sequence $\boldsymbol{n}_k$ is white zero-mean circularly symmetric Gaussian with $\mathbb{E}[\boldsymbol{n}_k \boldsymbol{n}_{k'}^*] = N_0 \delta_{k-k'} \mathbf{I}_{M_R}$, where $(\cdot)^*$ denotes Hermitian transpose, $\mathbf{I}_K$ is the $K \times K$ identity matrix, and the Kronecker delta function δ_k is unity when $k = 0$ and zero otherwise.

We assume Rayleigh fading with a potentially nonuniform power profile. A special case is when the channel is *spatially uncorrelated*, so that $\mathbf{G}_l = \sigma_l \mathbf{Q}_l$, where $\mathbf{Q}_l$ is an $M_R \times M_T$ matrix of independent and identically distributed (i.i.d.) $\mathcal{CN}(0,1)$ entries, in which $\mathcal{CN}(0,\sigma^2)$ denotes a complex random variable, whose real and imaginary parts are independent Gaussian random variables with zero mean and variance $\sigma^2/2$. The channel is normalized so that $\sum_{l=0}^{L} \sigma_l^2 = 1$. The power profile is called *uniform* when $\sigma_0^2 = \cdots = \sigma_L^2 = 1/(L+1)$. We also assume, for the sake of analysis simplicity, that the channel taps ($\{\mathbf{G}_l\}$) are also *temporally* uncorrelated, so that the elements in $\mathbf{G}_l$ are uncorrelated with the elements in $\mathbf{G}_{l'}$ when $l \neq l'$.

An effective strategy for dealing with the intersymbol interference (ISI) that results from frequency selectivity is to use OFDM [16], which leads to the MIMO-OFDM system illustrated in Fig. 1(a) [12]. The mth transmit antenna conveys a block of *information* symbols $\left\{u_1^{(m)}, \ldots, u_N^{(m)}\right\}$ by first taking the inverse discrete Fourier transform, which gives $\left\{x_1^{(m)}, \ldots, x_N^{(m)}\right\}$, adding a cyclic prefix of length L, and finally passing the sequence of $N + L$ symbols to a digital-to-analog converter and upconverter. The receiver downconverts and samples the signal at its mth antenna and removes the cyclic prefix, which gives $\left\{y_1^{(m)}, \ldots, y_N^{(m)}\right\}$. Taking the DFT yields $\left\{v_1^{(m)}, \ldots, v_N^{(m)}\right\}$. The net result is a bank of *memoryless* MIMO channels, one for each tone [12], [17], [18]:

$$\begin{aligned} \boldsymbol{v}_1 &= \mathbf{H}_1 \boldsymbol{u}_1 + \tilde{\boldsymbol{n}}_1 \\ &\vdots \quad \vdots \quad \vdots \\ \boldsymbol{v}_N &= \mathbf{H}_N \boldsymbol{u}_N + \tilde{\boldsymbol{n}}_N \end{aligned} \tag{2}$$

where $\boldsymbol{u}_n = \left[u_n^{(1)}, \ldots, u_n^{(M_T)}\right]^T$ is the vector of M_T information symbols transmitted at the nth tone, and where $\boldsymbol{v}_n = \left[v_n^{(1)}, \ldots, v_n^{(M_R)}\right]^T$ is the corresponding received vector. The equivalent MIMO-OFDM channel is shown in Fig. 1(b). The additive noise $\{\tilde{\boldsymbol{n}}_n\}$ in (2) is statistically identical to $\{\boldsymbol{n}_k\}$. The $M_R \times M_T$ matrix $\mathbf{H}_n$ represents the memoryless channel at the nth tone, where

$$\mathbf{H}_n = \sum_{l=0}^{L} \mathbf{G}_l e^{-j2\pi ln/N}. \tag{3}$$

For the special case of a memoryless channel ($L = 0$), $\mathbf{H}_n$ reduces to $\mathbf{G}_0$, independent of n, so that all tones see the same memoryless channel. We assert without proof the following about the statistics of $\{\mathbf{H}_n\}$.

Assertion 1: For spatially uncorrelated channels, the components of each $\mathbf{H}_n$ are i.i.d. $\mathcal{CN}(0,1)$.

Let $\{s_n^{(1)}, \ldots, s_n^{(M)}\}$ denote the positive ordered eigenvalues of $\mathbf{H}_n \mathbf{H}_n^*$, ordered so that $s_n^{(1)} \geq s_n^{(2)} \geq \cdots \geq s_n^{(M)} > 0$, where $M = \operatorname{rank}(\mathbf{H}_n)$. For spatially uncorrelated channels, $M = \min(M_T, M_R)$ is the minimum number of antennas at the two ends [19]. Let $\mathbf{H}_n = \mathbf{U}_n \mathbf{D}_n \mathbf{V}_n^*$ be a singular-value decomposition of the n-th memoryless MIMO channel, where $\mathbf{U}_n$ and $\mathbf{V}_n$ are $M_R \times M_R$ and $M_T \times M_T$ unitary matrices, respectively, and where $\mathbf{D}_n$ is an $M_R \times M_T$ diagonal matrix with diagonal components $\{(s_n^{(1)})^{\frac{1}{2}}, \ldots, (s_n^{(M)})^{\frac{1}{2}}\}$.

An *eigenbeamformer* [8], [20], [21] uses $\mathbf{V}_n$ as a prefilter for the n-th tone, as shown in Fig. 1(b), so that $\boldsymbol{u}_n = \mathbf{V}_n \boldsymbol{a}_n$ for some input vector $\boldsymbol{a}_n$. A matched-filter receiver (one that is matched to the cascade of the eigenbeamforming prefilters and the underlying MIMO-OFDM channel) then uses $\mathbf{U}_n^*$ as a receive filter for the n-th tone, as shown in Fig. 1(b), so that the output of the n-th such receive filter is $\boldsymbol{z}_n = \mathbf{U}_n^* \boldsymbol{v}_n$. Together, the eigenbeamforming and matched filtering transform the MIMO-OFDM channel of (2) into a bank of MN scalar

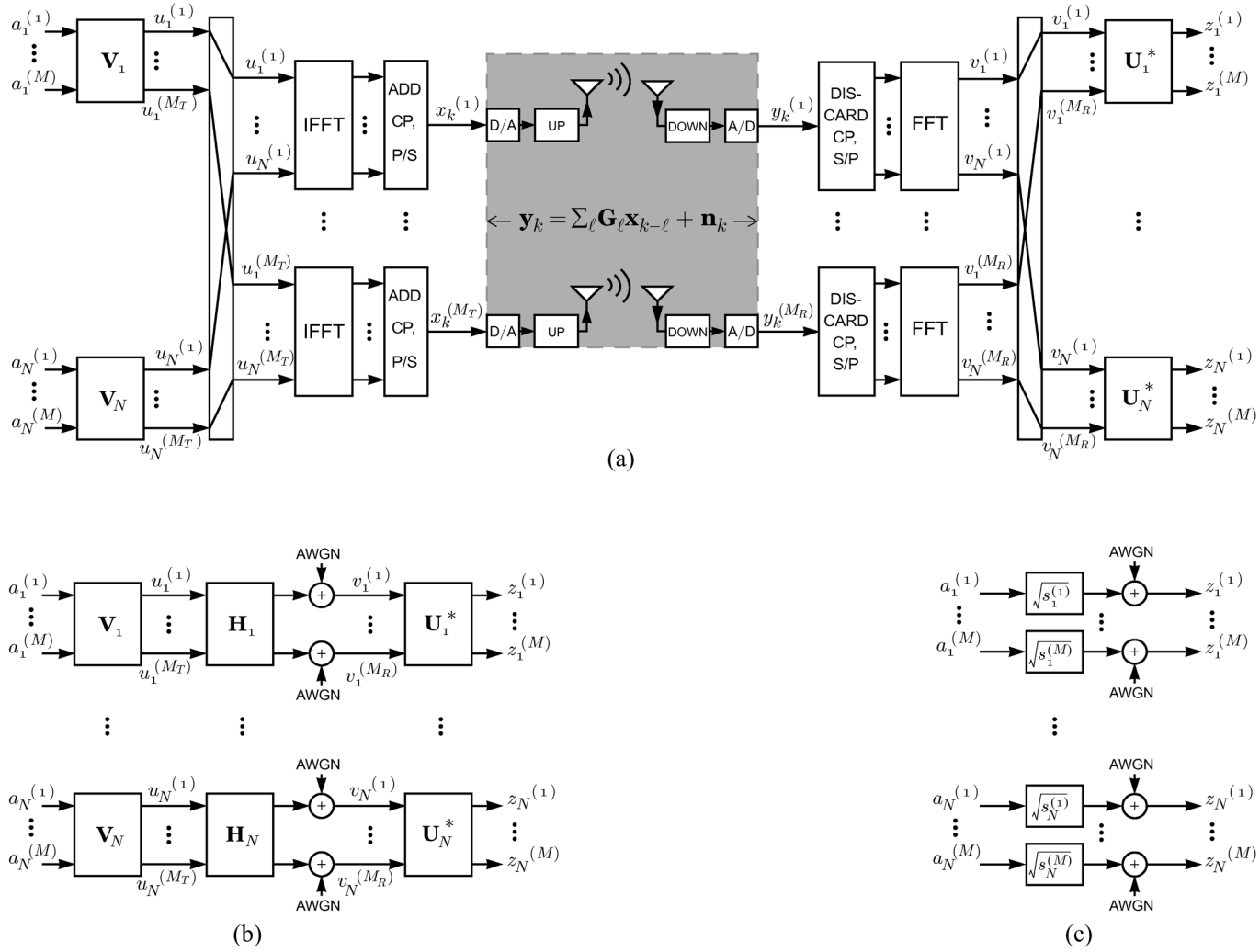

Fig. 1. (a) A MIMO-OFDM system with transmit and receive filters. (b) An equivalent discrete-time model for MIMO-OFDM on the left and MN scalar channels by eigenbeamforming on the right.

channels over space ($m = 1, 2, \ldots, M$) and frequency ($n = 1, 2, \ldots, N$) [12], such that

$$z_n^{(m)} = \sqrt{s_n^{(m)}}\, a_n^{(m)} + w_n^{(m)}, \quad \begin{matrix} n = 1, 2, \ldots, N \\ m = 1, 2, \ldots, M \end{matrix} \tag{4}$$

as illustrated in Fig. 1(c). The noise samples $\{w_n^{(m)}\}$ are i.i.d. $\mathcal{CN}(0, N_0)$, since the matrices $\{\mathbf{U}_n^*\}$ are unitary.

Note that, since the unitary eigenbeamforming and matched filtering do not decrease mutual information, the parallel scalar channels in (4) have the same mutual information as the MIMO-OFDM channel of (2). We should emphasize that the capacity of the effective MIMO-OFDM channel of (2) is strictly smaller than the capacity of the *underlying* frequency-selective MIMO channel of (1), since the use of the cyclic prefix at the transmitter (and discarding it at the receiver) incurs a loss of mutual information. This paper makes no attempt to quantify this loss in capacity, except to mention that it goes to zero as $N \to \infty$ [12]. Instead, our focus is on the capacity of the MIMO-OFDM channel in (2) itself.

In the model of (4), the eigenvalues $\{s_n^{(m)}\}$, which are random variables, play a key role in the capacity analysis. We define some useful functions of $\{s_n^{(m)}\}$. First, the empirical distribution of $\theta_n^{(m)} = s_n^{(m)}/M$ over an index set $\mathcal{L}$ for m and n is defined as

$$F_{\mathcal{L}}(x) = \frac{1}{|\mathcal{L}|} \sum_{(m,n)\in\mathcal{L}} 1\{\theta_n^{(m)} \le x\} \tag{5}$$

where $1\{\cdot\}$ is an indicator function, such that $1\{A\}$ is unity if the condition A is satisfied and zero otherwise, and where $|\mathcal{L}|$ denotes the cardinality of $\mathcal{L}$. Let

$$\mathcal{N}_u = \{(m,n); m = 1, 2, \ldots M \text{ and } n = 1, 2, \ldots N\} \tag{6}$$

indicate the *universe* index set, encompassing all m and n. Note that $F_{\mathcal{N}_u}(x)$ is a random function for a finite M. For flat fading ($L = 0$), however, $F_{\mathcal{N}_u}(x)$ converges to a nonrandom limit in distribution as $M \to \infty$ [6]. From Assertion 1, we deduce that $F_{\mathcal{N}_u}(x)$ also converges to a nonrandom limit when $L > 0$.

Other useful functions are arithmetic and geometric means of $\{s_n^{(m)}\}$ [16]. For a given index set $\mathcal{L}$, we define the arithmetic and geometric means of $\{s_n^{(m)}; (m,n) \in \mathcal{L}\}$ as

$$A_{\mathcal{L}} = \frac{1}{|\mathcal{L}|} \sum_{(m,n)\in\mathcal{L}} s_n^{(m)} \tag{7}$$

and

$$G_{\mathcal{L}} = \left(\prod_{(m,n)\in\mathcal{L}} s_n^{(m)} \right)^{1/|\mathcal{L}|} \tag{8}$$

respectively, both of which are also random. A well-known inequality is $A_{\mathcal{L}} \geq G_{\mathcal{L}}$ for any $\mathcal{L}$ with equality if and only if $s_n^{(m)}$ is independent of m and n over $\mathcal{L}$.

III. Power Allocation for MIMO-OFDM

We consider single-user communications over the parallel scalar channels of (4). Let $e_n^{(m)} = \mathbb{E}[|a_n^{(m)}|^2 | \{s_n^{(m)}\}]$ denote the energy of $a_n^{(m)}$ for the mth (space) and nth (frequency) scalar channel. For given $\{s_n^{(m)}\}$ and $\{e_n^{(m)}\}$, the maximum mutual information between $\{z_n^{(m)}\}$ and $\{a_n^{(m)}\}$ is [8]

$$I(\{s_n^{(m)}\}) = \frac{1}{N} \sum_{m=1}^{M} \sum_{n=1}^{N} \log_2 \left(1 + \frac{s_n^{(m)} e_n^{(m)}}{N_0} \right). \tag{9}$$

The units of $I(\{s_n^{(m)}\})$ are bits per signaling interval, which reduces to bits/sec/Hz when the rate loss due to the cyclic prefix is negligible. Since the channel is random, $I(\{s_n^{(m)}\})$ is also a random variable. We declare an outage occurrence when $I(\{s_n^{(m)}\})$ is smaller than the transmission rate R, and define the outage probability as $P_{\text{out}} = \text{Prob}[I(\{s_n^{(m)}\}) < R]$. We are interested in the maximum R that can be achieved with $P_{\text{out}} = 0$. In this context, the zero-outage capacity is defined as [8]

$$C_0 = \lim_{\epsilon \to 0} \sup_{\{e_n^{(m)}\}} \sup\{R; P_{\text{out}} \leq \epsilon\} \tag{10}$$

where the first supremum is over all $\{e_n^{(m)}\}$ satisfying an *average-energy* constraint:

$$\bar{E} = \mathbb{E}\left[\frac{1}{N} \sum_{n=1}^{N} \sum_{m=1}^{M} e_n^{(m)} \right]. \tag{11}$$

In terms of (11), the average SNR per receive antenna is simply $\bar{E}/N_0$.

The optimization in (10) is a power-allocation problem, where we find $\{e_n^{(m)}\}$ such that C_0 is maximized. The optimal choice of $\{e_n^{(m)}\}$ is obtained by solving [8] and [22]

$$\text{Minimize } \bar{E} = \mathbb{E}\left[\frac{1}{N} \sum_{n=1}^{N} \sum_{m=1}^{M} e_n^{(m)} \right]$$
$$\text{Subject to } \frac{1}{N} \sum_{n=1}^{N} \sum_{m=1}^{M} \log_2 \left(1 + \frac{s_n^{(m)} e_n^{(m)}}{N_0} \right) = R \tag{12}$$

as described in the following theorem.

Theorem 1 (From [8]): The optimal power allocation is given by $e_n^{(m)} = N_0\{\lambda - 1/s_n^{(m)}\}^+$, with $\{x\}^+ = \max(0, x)$, where

$$\lambda = \frac{2^{RN/|\mathcal{M}|}}{G_{\mathcal{M}}} \tag{13}$$

ensures that $I(\{s_n^{(m)}\}) = R$ is satisfied, and where the index set $\mathcal{M}$ in (13) identifies the *used* channels according to $\mathcal{M} = \{(m,n) : \lambda s_n^{(m)} \geq 1\}$.

Proof: See [8]. □

In Theorem 1, the average energy requirement $\bar{E}$ is a function of R, that is, $\bar{E} = f(R)$. The zero-outage capacity at an SNR of $\bar{E}/N_0$ is then obtained by inverting this function, $C_{0,\text{OPT}} = f^{-1}(\bar{E})$. Generally, $C_{0,\text{OPT}}$ is positive if $\mathbb{E}[1/G_{\mathcal{N}_u}] < \infty$ [8], where $\mathcal{N}_u$ denotes the universe index set in (6). When $L = 0$, $C_{0,\text{OPT},L=0}$ corresponds to the zero-outage capacity of a flat-fading MIMO channel.

The solution in Theorem 1 requires performing water-filling over MN channels, and thus its computational complexity can be high, especially when MN is very large. This motivates us to find reduced-complexity allocation strategies. We reduce complexity by applying two stricter constraints when solving the allocation problem: the *frequency-uniform-spectral-efficiency* and *fixed-rate* constraints.

A. FUSE Allocation

We first introduce the frequency-uniform-spectral-efficiency (FUSE) constraint. Unlike the original constraint of (12), which requires only that the *average* spectral efficiency (averaged over the N tones) is equal to the target value R, the FUSE forces the spectral efficiency to be R at each tone. With the FUSE constraint, the problem becomes

$$\text{Minimize } \bar{E} = \mathbb{E}\left[\frac{1}{N} \sum_{n=1}^{N} \sum_{m=1}^{M} e_n^{(m)} \right]$$
$$\text{Subject to } \sum_{m=1}^{M} \log_2 \left(1 + \frac{s_n^{(m)} e_n^{(m)}}{N_0} \right) = R \text{ for each } n. \tag{14}$$

Proposition 1 (FUSE Allocation): The power allocation that solves (14) is $e_n^{(m)} = N_0\{\mu_n - 1/s_n^{(m)}\}^+$, where

$$\mu_n = \frac{2^{R/|\mathcal{M}_n|}}{G_{\mathcal{M}_n}} \tag{15}$$

ensures that $\sum_{m=1}^{M} \log_2(\mu_n s_n^{(m)}) = R$ is satisfied for all n, and where $\mathcal{M}_n = \{(m,n); \mu_n s_n^{(m)} \geq 1\}$ is the index set of the *used* channels for the nth tone.

Proof: From (14), the objective function can be rewritten as

$$\mathbb{E}\left[\frac{1}{N} \sum_{n=1}^{N} \sum_{m=1}^{M} e_n^{(m)} \right] = \frac{1}{N} \sum_{n=1}^{N} \mathbb{E}\left[\sum_{m=1}^{M} e_n^{(m)} \right]. \tag{16}$$

With the FUSE constraint, the problem reduces to N independent smaller problems

$$\begin{aligned} &\text{Minimize } \mathbb{E}\left[\sum_{m=1}^{M} e_n^{(m)}\right] \\ &\text{Subject to } \sum_{m=1}^{M} \log_2\left(1+\frac{s_n^{(m)} e_n^{(m)}}{N_0}\right) = R \end{aligned} \quad \text{for all } n. \tag{17}$$

For each n, the optimal $\{e_n^{(m)}\}$ is in the same form of Theorem 1, where μ_n and $\mathcal{M}_n$ correspond to λ and $\mathcal{M}$ in Theorem 1, respectively, for each n. □

Inverting $\bar{E}$ with the optimal $\{e_n^{(m)}\}$ of Proposition 1 with respect to R, we obtain $C_{0,\mathrm{FUSE}}$, the zero-outage capacity with the FUSE constraint. To achieve $C_{0,\mathrm{FUSE}}$, we perform water-filling over M scalar channels independently, N times. In contrast, to achieve $C_{0,\mathrm{OPT}}$ requires water-filling jointly over the MN scalar channels. The FUSE constraint reduces complexity considerably when N is large. However, this complexity reduction leads to a capacity loss, such that $C_{0,\mathrm{FUSE}} \le C_{0,\mathrm{OPT}}$. In the following, we attempt to quantify this loss.

Proposition 2: The FUSE allocation is asymptotically lossless as the number of antennas gets large, in the sense that $C_{0,\mathrm{FUSE}} \to C_{0,\mathrm{OPT}}$ as $M \to \infty$.

Proof: The proof is based on the fact that the power allocation is associated with the empirical distribution of $\{s_n^{(m)}\}$ in (5). If two systems have the same empirical distribution for all channel realizations, they achieve the same zero-outage capacity. Consider two index sets: the universe index set $\mathcal{N}_u$ in (6) for $C_{0,\mathrm{OPT}}$, and the *spatial* index set

$$\mathcal{N}_s = \{(m,n); m = 1,2,\ldots,M \text{ for a specific } n\} \tag{18}$$

for $C_{0,\mathrm{FUSE}}$. When M is finite, the empirical distribution functions for $\mathcal{N}_u$ and $\mathcal{N}_s$ are different, $F_{\mathcal{N}_u}(x) \neq F_{\mathcal{N}_s}(x)$. However, when N approaches infinity, we have $F_{\mathcal{N}_u}(x) = F_{\mathcal{N}_s}(x)$ from [23], and therefore both $\mathcal{N}_u$ and $\mathcal{N}_s$ achieve the same zero-outage capacity. □

Proposition 2 suggests that the penalty of the FUSE allocation converges to zero as M grows. It is an encouraging result to justify the use of the FUSE allocation, but we are more interested in its performance at a finite M. We will show that the convergence in Proposition 2 is fast by high-SNR analysis in Section IV and experimental results in Section V.

B. FIXED Allocation

The FUSE constraint forces each tone to have the same spectral efficiency, but it allows for some adaptation within the spatial channels of each tone. We now introduce the *fixed-rate (FIXED)* constraint, which takes this one step further: it fixes the rate $r_n^{(m)} = \log_2(1 + s_n^{(m)} e_n^{(m)}/N_0)$ allocated to each scalar channel, regardless of $\{s_n^{(m)}\}$. The rate allocation is deterministic and nonadaptive, and is independent of the particular fading realization. Once the rates $\{r_n^{(m)}\}$ are specified, the power allocation may be simply calculated from a closed-form formula, $e_n^{(m)} = N_0(2^{r_n^{(m)}} - 1)/s_n^{(m)}$, and thus no dynamic water-filling is needed. We should emphasize that the FIXED constraint does not mean that $\{r_n^{(m)}\}$ are uniform for all m and n. Instead, the rates $\{r_n^{(m)}\}$ are optimized to the anticipated fading statistics so as to minimize the average required energy $\bar{E}$. Before presenting the optimal rate allocation, we define the number of *available* scalar channels with the FIXED constraint.

Definition 1: Let $\tilde{M}$ be the largest integer satisfying $\mathbb{E}[1/s_n^{(\tilde{M})}] < \infty$ for each n. We may interpret $\tilde{M}$ as the number of scalar channels per tone that can convey data at a nonzero rate with a FIXED allocation.

If a nonzero rate were allocated to (m,n) with $\mathbb{E}[1/s_n^{(m)}] \to \infty$, the average energy requirement would be infinite. For this reason, we avoid using such scalar channels. From Assertion 1, $\tilde{M}$ is identical for all n. Then, the allocation problem with the FIXED constraint is to find $\{r_n^{(m)}\}$ such that

$$\begin{aligned} &\text{Minimize } \bar{E} = \mathbb{E}\left[\frac{1}{N}\sum_{n=1}^{N}\sum_{m=1}^{M}\frac{2^{r_n^{(m)}}-1}{s_n^{(m)}/N_0}\right] \\ &\text{Subject to } \frac{1}{N}\sum_{n=1}^{N}\sum_{m=1}^{M} r_n^{(m)} = R \end{aligned} \tag{19}$$

where $\{r_n^{(m)}\}$ are independent of $\{s_n^{(m)}\}$.

Proposition 3 (FIXED Allocation): The optimal choice of $\{r_n^{(m)}\}$ that minimizes $\bar{E}$ is

$$r_n^{(m)} = \left\{\log_2\left(\frac{\nu}{\mathbb{E}[1/s_n^{(m)}]}\right)\right\}^+ \tag{20}$$

where

$$\nu = \frac{2^{R/|\mathcal{M}_{\mathrm{FIXED}}|}}{\Gamma_{\mathcal{M}_{\mathrm{FIXED}}}} \tag{21}$$

ensures that $\frac{1}{N}\sum_{n=1}^{N}\sum_{m=1}^{M} r_n^{(m)} = R$ is satisfied, and where

$$\mathcal{M}_{\mathrm{FIXED}} = \{(m,n); \nu/\mathbb{E}[1/s_n^{(m)}] \ge 1\} \tag{22}$$

is the index set for used channels out of $\tilde{M}$ channels for each n. In (21) and (22), $\Gamma_{\mathcal{M}_{\mathrm{FIXED}}}$ denotes the geometric mean of $1/\mathbb{E}[1/s_n^{(m)}]$ over $\mathcal{M}_{\mathrm{FIXED}}$, namely

$$\Gamma_{\mathcal{M}_{\mathrm{FIXED}}} = \left(\prod_{(m,n)\in\mathcal{M}_{\mathrm{FIXED}}} 1/\mathbb{E}[1/s_n^{(m)}]\right)^{1/|\mathcal{M}_{\mathrm{FIXED}}|}. \tag{23}$$

Proof: Since $\{r_n^{(m)}\}$ are independent of $\{s_n^{(m)}\}$, the objective function in (19) becomes

$$\frac{\bar{E}}{N_0} = \mathbb{E}\left[\frac{1}{N}\sum_{n=1}^{N}\sum_{m=1}^{M}\frac{2^{r_n^{(m)}}-1}{s_n^{(m)}}\right] = \frac{1}{N}\sum_{n=1}^{N}\sum_{m=1}^{\tilde{M}}\frac{(2^{r_n^{(m)}}-1)}{g_n^{(m)}} \tag{24}$$

where $g_n^{(m)} = 1/\mathbb{E}[1/s_n^{(m)}]$. In (24), $\{g_n^{(m)}\}$ work as the squared channel gains, and each tone has $\tilde{M}$ scalar channels. Since $\{g_n^{(1)},\ldots,g_n^{(\tilde{M})}\}$ is identical for all n from Assertion 1, the problem reduces to water-filling over $\tilde{M}$ scalar channels, such that ν is the water-level parameter and $\mathcal{M}_{\mathrm{FIXED}}$ is the index set for used channels. The geometric mean $\Gamma_{\mathcal{M}_{\mathrm{FIXED}}}$ replaces $G_{\mathcal{M}_n}$ of Proposition 1 in this case. □

From Proposition 3, we can confirm that $\{r_n^{(m)}\}$ are deterministic, obtained from performing water-filling over deterministic channels, $\{1/\mathbb{E}[1/s_n^{(m)}]\}$. Thus, we only need to know $\{1/\mathbb{E}[1/s_n^{(m)}]\}$, not all statistics of $\{s_n^{(m)}\}$, to decide $\{r_n^{(m)}\}$. Once $\{r_n^{(m)}\}$ are predetermined, the optimal power allocation is simply calculated by

$$e_n^{(m)} = \frac{2^{r_n(m)}-1}{s_n^{(m)}/N_0} = N_0\left\{\frac{\nu}{s_n^{(m)}\mathbb{E}[1/s_n^{(m)}]} - \frac{1}{s_n^{(m)}}\right\}^+ \quad (25)$$

for each realization of $\{s_n^{(m)}\}$. The fact that the required energy $\{e_n^{(m)}\}$ is a function of $\{s_n^{(m)}\}$ indicates that the FIXED allocation requires an *adaptive* power allocation, even though it uses a nonadaptive rate allocation. In other words, the FIXED allocation combines a fixed rate allocation with adaptive power control to avoid an outage.

Corollary 1: The FIXED constraint implies the FUSE constraint in the sense that $\sum_{m=1}^{M} r_n^{(m)} = R$ for all n.

Proof: In the proof of Proposition 3, we already showed that the rate allocation is independent of n. □

Complexity reduction is remarkable with the FIXED allocation, but fixing rate allocation could incur a significant penalty. Let $C_{0,\mathrm{FIXED}}$ denote the zero-outage capacity with the FIXED allocation. Since the FIXED constraint is stricter than the FUSE constraint, we have $C_{0,\mathrm{OPT}} \geq C_{0,\mathrm{FUSE}} \geq C_{0,\mathrm{FIXED}}$. The fact that $\tilde{M}$ is smaller than $\leq M$ can seriously decrease the zero-outage capacity, as will be discussed in Section IV. When M is sufficiently large, however, the performance degradation is not critical. As M tends to infinity, we have the following proposition.

Proposition 4: The FIXED allocation is asymptotically lossless as the number of antennas gets large, in the sense that $C_{0,\mathrm{FIXED}} \to C_{0,\mathrm{OPT}}$ as $M \to \infty$.

Proof: Let $\theta_n^{(m)} = s_n^{(m)}/M$ and let $\mathcal{N}_s$ be the spatial index set in (18). From Proposition 3, $C_{0,\mathrm{FIXED}}$ depends on the empirical distribution of $1/\mathbb{E}[1/\theta_n^{(m)}]$

$$V_{\mathcal{N}_s}(x) = \frac{1}{|\mathcal{N}_s|}\sum_{m=1}^{M} 1\left\{1/\mathbb{E}[1/\theta_n^{(m)}] \leq x\right\} \quad (26)$$

if including $1/\mathbb{E}[1/\theta_n^{(m)}] = 0$, which is identical for all n. The goal is to show that $V_{\mathcal{N}_s}(x)$ is equal to $F_{\mathcal{N}_s}(x)$, the empirical distribution for $\{s_n^{(m)}\}$ in (5), as $M \to \infty$. When $M \to \infty$, $F_{\mathcal{N}_s}(x)$ becomes nonrandom, and thus $1\{\theta_n^{(m)} \leq x\} = \mathbb{E}[\{\theta_n^{(m)} \leq x\}] = \mathrm{Prob}[\theta_n^{(m)} \leq x]$, implying that the density function of $\theta_n^{(m)}$ is a delta function at $\theta_n^{(m)}$. Therefore, $1/\mathbb{E}[1/\theta_n^{(m)}] = \theta_n^{(m)}$. If $1/\mathbb{E}[1/\theta_n^{(m)}] = 0$, this corresponds to $\theta_n^{(m)} = 0$. Therefore, by substituting $1/\mathbb{E}[1/\theta_n^{(m)}] = \theta_n^{(m)}$ into (5), we obtain $V_{\mathcal{N}_s}(x) = F_{\mathcal{N}_s}(x)$ for infinite M. Therefore, $C_{0,\mathrm{FIXED}}$ converges to $C_{0,\mathrm{FUSE}}$ as $M \to \infty$ sine $V_{\mathcal{N}_s}(x)$ and $F_{\mathcal{N}_s}(x)$ account for $C_{0,\mathrm{FIXED}}$ and $C_{0,\mathrm{FUSE}}$, respectively. From Proposition 2, we deduce that $C_{0,\mathrm{FIXED}}$ is asymptotically identical to $C_{0,\mathrm{OPT}}$ as $M \to \infty$. □

We showed in Proposition 2 that water-filling over spatial channels is sufficient to approach $C_{0,\mathrm{OPT}}$. Furthermore, Proposition 4 illustrates that even a nonadaptive rate allocation can achieve $C_{0,\mathrm{OPT}}$. In other words, water-filling is not necessary to approach $C_{0,\mathrm{OPT}}$ in MIMO-OFDM. Note that the FIXED allocation must be matched to channel statistics, while the FUSE allocation is independent of statistics.

For flat-fading channels ($L = 0$), Proposition 4 implies that the spatial rate allocation can be predetermined according to channel statistics and fixed for all channel uses without incurring any penalty. This optimality of the FIXED allocation can be explained by the fact that MIMO channels tend to lose their randomness as the size of MIMO channel grows.

IV. Asymptotic Behavior at High SNR

We have seen that both the FUSE and FIXED allocations do not incur any capacity loss when $M \to \infty$, but it is of obvious practical interest to know how these allocation strategies perform when M is finite. As water-filling is a complicated process, it is difficult to analyze the zero-outage capacity directly. For this reason, we instead examine the asymptotic behavior at high SNR. First of all, in the case of the optimal power allocation in Theorem 1, we have the following result:

Theorem 2 (From [8]): As SNR tends to infinity, $C_{0,\mathrm{OPT}}$ asymptotically approaches

$$C_{0,\mathrm{OPT}} \to M\log_2\left(\frac{\bar{E}/N_0}{M\mathbb{E}[1/G_{\mathcal{N}_u}]}\right) \quad (27)$$

as long as $\mathbb{E}[1/G_{\mathcal{N}_u}] < \infty$, where $\mathcal{N}_u$ is the universe index set in (6) and $\bar{E}/N_0$ is the SNR.

Proof: See [8]. □

The capacity increase provided by a MIMO system is often quantified by the spatial multiplexing gain [24], [25], defined as the limit of the ratio $C_{0,\mathrm{OPT}}/\log_2(\bar{E}/N_0)$ as SNR goes to infinity. Theorem 2 tells us that this gain is equal to M, independent of L. Nevertheless, L does have an impact on $C_{0,\mathrm{OPT}}$, since $1/\mathbb{E}[1/G_{\mathcal{N}_u}]$ in (27) is a function of L. In this context, $1/\mathbb{E}[1/G_{\mathcal{N}_u}]$ is an important factor to understand the impact of L on $C_{0,\mathrm{OPT}}$, but difficult to evaluate analytically. We resort to Monte-Carlo simulations to evaluate $1/\mathbb{E}[1/G_{\mathcal{N}_u}]$ as summarized in Fig. 2 for $L \in \{0,1,\ldots,5\}$ and $M \in \{2,4,6\}$ by averaging over 10,000 $M \times M$ Rayleigh independent channels with the uniform power profile. Fig. 2 clearly shows that $1/\mathbb{E}[1/G_{\mathcal{N}_u}]$ is an increasing function of L, meaning that $C_{0,\mathrm{OPT}}$ is also increasing with L, and converges as L grows.

It would still be nice to have a closed-form formula for $1/\mathbb{E}[1/G_{\mathcal{N}_u}]$ to understand the behaviors of $C_{0,\mathrm{OPT}}$ better. We are also interested in what would happen when $L \to \infty$. Does $C_{0,\mathrm{OPT}}$ increase without a bound when $L \to \infty$? How fast does the penalty of the FUSE allocation converge to zero as $M \to \infty$? To answer these questions, we use arithmetic mean, instead of geometric mean, to derive a closed-form bound as follows.

Proposition 5: The asymptote of $C_{0,\mathrm{OPT}}$ in (27) is bounded by

$$C_{0,\mathrm{OPT}} \leq M\log_2\left(\frac{\bar{E}/N_0}{M\mathbb{E}[1/A_{\mathcal{N}_u}]}\right). \quad (28)$$

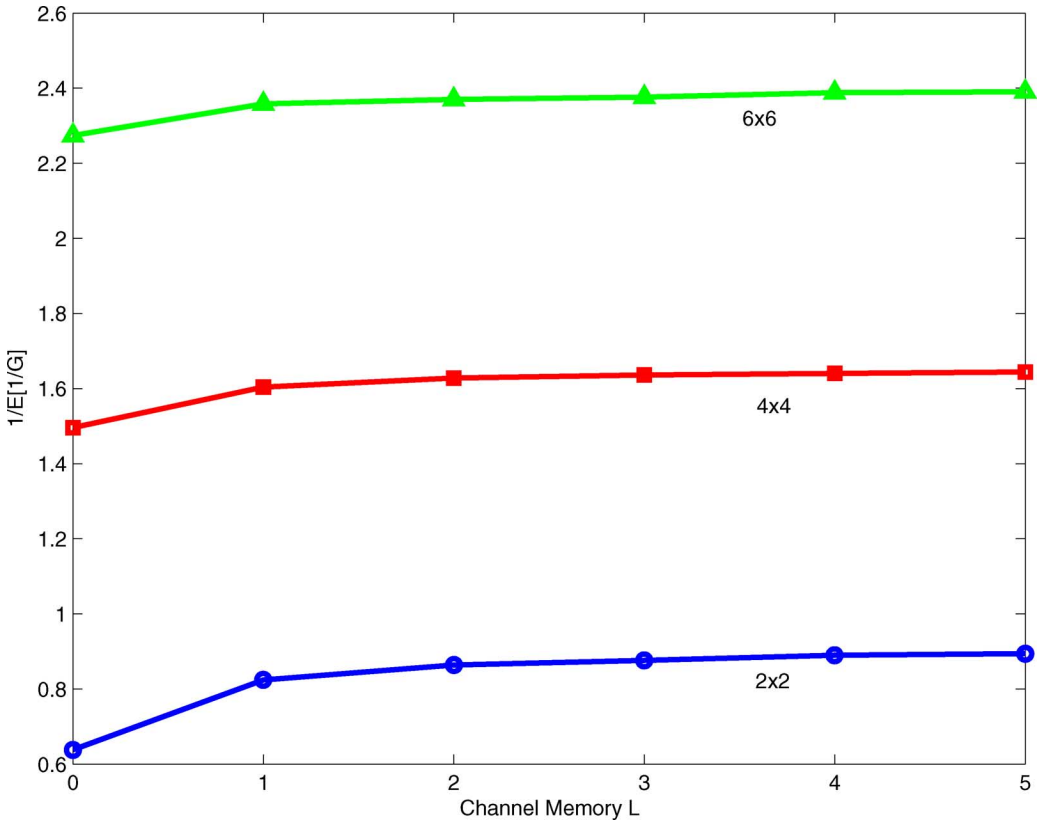

Fig. 2. $1/\mathbb{E}[1/G_{\mathcal{N}_u}]$ for $M \times M$ Rayleigh-fading channels with channel memory L by Monte Carlo simulations.

For spatially uncorrelated channels, the bound in (28) is maximized for the uniform power profile, that is $\sigma_0^2 = \cdots = \sigma_L^2 = 1/(L+1)$, for which $1/\mathbb{E}[1/A_{\mathcal{N}_u}]$ in (28) can be evaluated as

$$\frac{1}{\mathbb{E}[1/A_{\mathcal{N}_u}]} = \frac{M_T M_R(L+1)-1}{M(L+1)}. \tag{29}$$

Proof: Deferred to Appendix A. □

From Proposition 5, the first question is clearly answered; as $L \to \infty$ for finite M and $\bar{E}/N_0$, the bound in (28) is finite such that it converges

$$M\log_2\left(\frac{M_T M_R(L+1)-1}{M^2(L+1)}\frac{\bar{E}}{N_0}\right) \to M\log_2\left(\frac{\max(M_T,M_R)}{\min(M_T,M_R)}\frac{\bar{E}}{N_0}\right). \tag{30}$$

Therefore, $C_{0,\mathrm{OPT}}$ also converges to a finite value for infinite L. This means that the gain from frequency selectivity ($L > 0$), compared to flat fading ($L = 0$), is limited. The increase by L results in the capacity penalty of the FUSE allocation, meaning that the penalty is finite.

On the other hand, to investigate the convergence speed of the FUSE allocation in Proposition 2, we derive the following corollary from Proposition 5.

Corollary 2: As SNR tends to infinity, $C_{0,\mathrm{FUSE}}$ asymptotically approaches

$$C_{0,\mathrm{FUSE}} \to M\log_2\left(\frac{\bar{E}/N_0}{M\mathbb{E}[1/G_{\mathcal{N}_s}]}\right) \le M\log_2\left(\frac{\bar{E}/N_0}{M\mathbb{E}[1/A_{\mathcal{N}_s}]}\right) \tag{31}$$

where $\mathcal{N}_s$ is the spatial index set in (18). From Assertion 1, $G_{\mathcal{N}_s}$ is equal to $G_{\mathcal{N}_{u,L=0}}$ with the universe index set $\mathcal{N}_u$ in (6). With the uniform power profile, $1/\mathbb{E}[1/G_{\mathcal{N}_s}]$ is upper-bounded by $1/\mathbb{E}[1/A_{\mathcal{N}_{u,L=0}}] = (M_T M_R - 1)/M$.

Proof: The proof is straightforward since $C_{0,\mathrm{FUSE}} = C_{0,\mathrm{OPT},L=0}$ from Proposition 1. □

Corollary 2 shows that the spatial multiplexing gain of the FUSE allocation is also linearly proportional to M, but $C_{0,\mathrm{FUSE}}$ has $1/\mathbb{E}[1/G_{\mathcal{N}_s}]$ in the logarithm instead of $1/\mathbb{E}[1/G_{\mathcal{N}_u}]$, which results in a SNR penalty. We define the SNR penalty of the FUSE allocation relative to the optimal allocation in Theorem 1 as

$$\text{SNR penalty} = \frac{1/\mathbb{E}[1/G_{\mathcal{N}_u}]}{1/\mathbb{E}[1/G_{\mathcal{N}_s}]} \approx \frac{1/\mathbb{E}[1/A_{\mathcal{N}_u}]}{1/\mathbb{E}[1/A_{\mathcal{N}_s}]} \tag{32}$$

which accounts for the additional SNR required by the FUSE allocation over the optimal allocation at high SNR. The SNR penalty is approximated by replacing the geometric mean with the arithmetic mean, as described in (32). Note that the approximate SNR penalty in (32) is maximized for the uniform power profile in case of uncorrelated channels, for which the approximate penalty can be evaluated into a closed-form formula:

$$\text{SNR penalty} \approx \frac{M_T M_R(L+1)-1}{(M_T M_R - 1)(L+1)}. \tag{33}$$

Thus, it is the uniform power profile that incurs the largest SNR penalty in the FUSE allocation, which is a function of the channel memory (L) and the number of antennas (M_T and M_R). According to computer simulations, the uniform power profile also maximizes the exact SNR penalty in (32), but no analytic proof has been found.

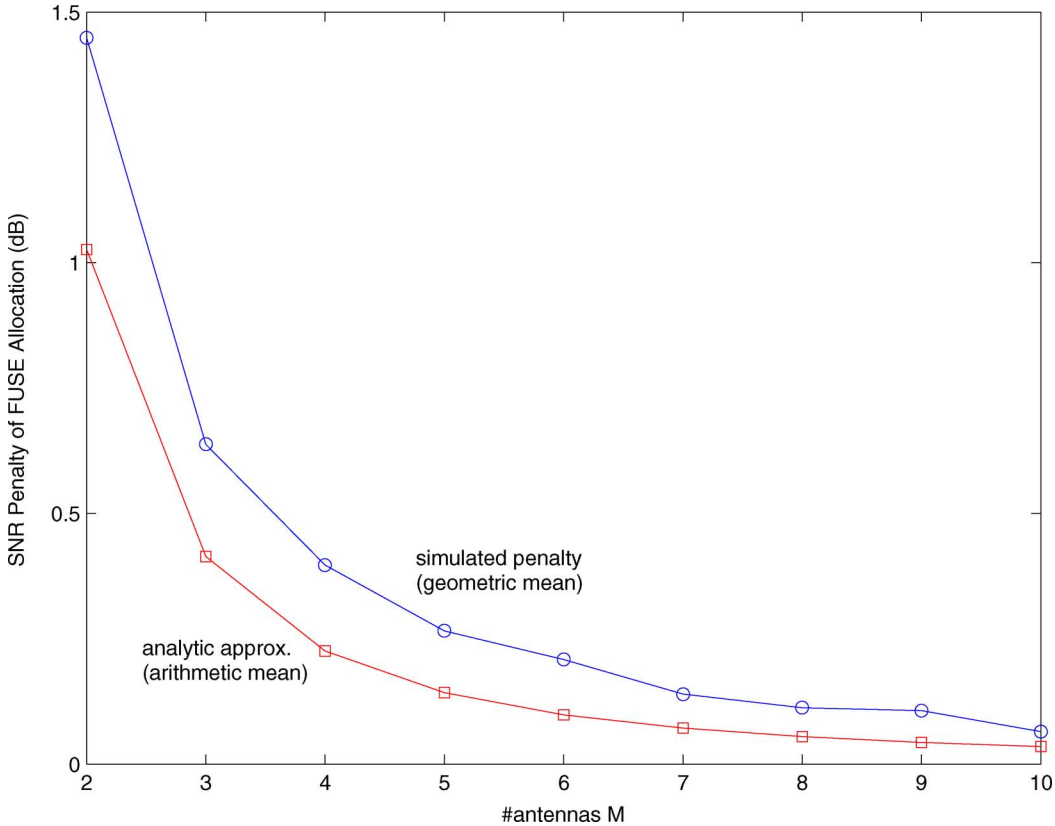

Fig. 3. SNR penalty at high SNR due to the FUSE constraint, as a function of M, when $L = 4$. The approximation by arithmetic mean (squares) is from (33), while the actual SNR penalty (circles) evaluate (32) using Monte Carlo simulations.

It should be noted that the approximation in (32) uses the bounds of $C_{0,\mathrm{OPT}}$ and $C_{0,\mathrm{FUSE}}$, which could be totally misleading. However, we can confirm that the behaviors of (33) well match what is expected. For instance, the approximate penalty becomes 0 dB (no penalty) when either $L = 0$ or $M \to \infty$. The result for $M \to \infty$ agrees with Proposition 2. When $L \to \infty$, it converges to $M_T M_R/(M_T M_R - 1)$, that is, the penalty is bounded.

To verify the validness of the approximation in (33) for finite M and L, Fig. 3 illustrates the SNR penalty in (32) and its approximation in (33) for a square MIMO channel ($M_T = M_R = M$) with $L = 4$ as M ranges from 1 to 10. For the actual SNR penalty in (32), we used Monte Carlo simulations by averaging over 10 000 independent Rayleigh-fading channels. In Fig. 3, we can observe that the approximation is slightly smaller than the actual SNR penalty, but both clearly demonstrates that the penalty approaches quickly to 0 dB. In other words, $C_{0,\mathrm{FUSE}}$ quickly converges to $C_{0,\mathrm{OPT}}$ as $M \to \infty$.

Finally, the following proposition shows the asymptotic behaviors of the FIXED allocation.

Proposition 6: As SNR tends to infinity

$$C_{0,\mathrm{FIXED}} \to \tilde{M} \log_2 \left(\frac{\bar{E}/N_0}{\tilde{M}/\Gamma_{\tilde{\mathcal{N}}}} \right) \tag{34}$$

where

$$\Gamma_{\tilde{\mathcal{N}}} = \left(\prod_{(m,n)\in\tilde{\mathcal{N}}} \frac{1}{\mathbb{E}[1/s_n^{(m)}]} \right)^{1/\tilde{M}} \tag{35}$$

is the geometric mean of $1/\mathbb{E}[1/s_n^{(m)}]$ over $\tilde{\mathcal{N}} = \{(m,n); m = 1, 2, \ldots, \tilde{M} \text{ for a specific } n\}$, and where $\tilde{M}$ is defined in Definition 1.

Proof: Deferred to Appendix B. □

Proposition 6 shows that $C_{0,\mathrm{FIXED}}/\log(\bar{E}/N_0)$ is asymptotically proportional to $\tilde{M}$ rather than M. For some types of fading, $\tilde{M}$ can be smaller than M, which means that the FIXED allocation incurs a lower spatial multiplexing gain. The difference in spatial multiplexing gain leads to an infinite penalty as SNR grows. For example, when the channel is spatially uncorrelated Rayleigh fading and square ($M = M_T = M_R$), $\tilde{M}$ is at most $M - 1$ since $s_n^{(M)}$ is exponential distributed and $\mathbb{E}[1/s_n^{(M)}]$ diverges [26]. We conjecture, from computer simulations, that $\tilde{M} = M - 1$ for any $M \times M$ channel though we can only prove this for small M by explicitly calculating $\mathbb{E}[1/s_n^{(m)}]$ from the marginal distribution of $\{s_n^{(m)}\}$ [27]. On the other hand, when the channel is nonsquare ($M_T \neq M_R$), we have $\tilde{M} = M = \min(M_T, M_R)$ as deduced from [26], and the FUSE allocation has the same spatial multiplexing gain as the optimal allocation in the sense that $C_{0,\mathrm{FIXED}}/\log(\bar{E}/N_0)$ is equal to $C_{0,\mathrm{OPT}}/\log(\bar{E}/N_0)$.

V. Numerical Results

We have investigated three power-allocation strategies for MIMO-OFDM with eigenbeamforming as follows:

- optimal allocation (Theorem 1);
- FUSE allocation (Proposition 1);
- FIXED allocation (Proposition 3);

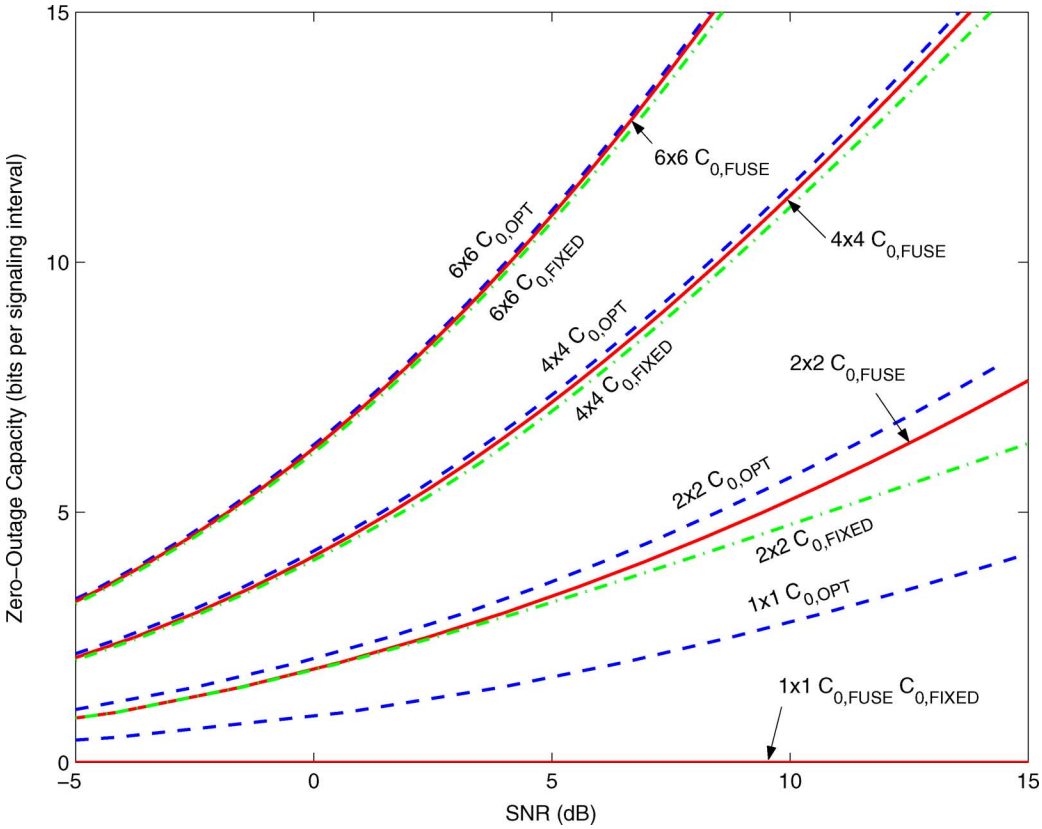

Fig. 4. Zero-outage capacities in bits per signaling interval for the optimal power allocation, the FUSE allocation, and the FIXED allocation for $L = 4$.

which achieve $C_{0,\mathrm{OPT}}$, $C_{0,\mathrm{FUSE}}$, and $C_{0,\mathrm{FIXED}}$, respectively. It has been shown that both $C_{0,\mathrm{FUSE}}$ and $C_{0,\mathrm{FIXED}}$ converge to $C_{0,\mathrm{OPT}}$ as the antenna array size tends to infinity. In this section, we show via Monte Carlo simulations that $C_{0,\mathrm{FUSE}}$ and $C_{0,\mathrm{FIXED}}$ are nearly optimal for moderate antenna array sizes. Monte Carlo simulations generated 10 000 independent sets of square channels ($M_T = M_R = M$) with the uniform power profile. We assume that OFDM has $N = 256$ tones.

A. *Spatially Uncorrelated Channels*

Fig. 4 shows $C_{0,\mathrm{OPT}}$, $C_{0,\mathrm{FUSE}}$, and $C_{0,\mathrm{FIXED}}$ against SNR in dB for $L = 4$ and $M \in \{1, 2, 4, 6\}$ when the fading is spatially uncorrelated as described in Section II. When $M = 1$ (SISO), both $C_{0,\mathrm{FUSE}}$ and $C_{0,\mathrm{FIXED}}$ are zero, as reported in [2]. The optimal allocation has nonzero $C_{0,\mathrm{OPT}}$ because water-filling across tones exploits the frequency diversity from channel memory, otherwise it too would be zero. In stark contrast, when $M = 2$, $C_{0,\mathrm{FUSE}}$ and $C_{0,\mathrm{FIXED}}$ become nonzero due to spatial (antenna) diversity. As explained in Section IV, $C_{0,\mathrm{OPT}}$ and $C_{0,\mathrm{FUSE}}$ have the same asymptotic slope, i.e., spatial multiplexing gain ($M = 2$), while $C_{0,\mathrm{FIXED}}$ has a lower slope ($\tilde{M} = 1$). Thus, it can be seen that the gap between $C_{0,\mathrm{FIXED}}$ and $C_{0,\mathrm{OPT}}$ grows with SNR, and the FIXED constraint incurs an unbounded penalty in the end as SNR tends to infinity. As the antenna array sizes increase to $M = 4$ and $M = 6$, both $C_{0,\mathrm{FUSE}}$ and $C_{0,\mathrm{FIXED}}$ are very close to $C_{0,\mathrm{OPT}}$, as expected from Fig. 3. Even for $M = 4$ or $M = 6$, $C_{0,\mathrm{FIXED}}$ has a lower asymptotic slope ($\tilde{M} = M - 1$) than $C_{0,\mathrm{OPT}}$ or $C_{0,\mathrm{FUSE}}$, and eventually incurs an unbounded penalty as SNR goes to infinity. However, for a range of practical SNR, Fig. 4 illustrates the penalty of the FIXED allocation is small.

To emphasize how far $C_{0,\mathrm{FUSE}}$ and $C_{0,\mathrm{FIXED}}$ are separated from $C_{0,\mathrm{OPT}}$, Fig. 5 illustrates the SNR penalty, which is the additional SNR required by the FUSE and FIXED allocations relative to the optimal allocation at a given transmission rate R ranging from 2 to 14 bits per signaling interval. The SNR penalty corresponds to horizontal separation from $C_{0,\mathrm{OPT}}$ in Fig. 4. The FUSE allocation incurs an SNR penalty of more than 0.8 dB for $M = 2$, but the penalty reduces to less than 0.3 dB for $M = 4$ and $M = 6$. From Fig. 3, the SNR penalties converge to $\{1.47, 0.41, 0.20\}$ in decibels for $M \in \{2, 4, 6\}$, respectively, as R goes to infinity. For FIXED allocation, the SNR penalty at $M = 2$ is quite large due to a shallower slope of $C_{0,\mathrm{FIXED}}$ (i.e., smaller multiplexing gain, $\tilde{M} = 1$). Fig. 5(b) illustrates that the penalty is more than 1 dB and quickly diverges. For $M = 4$ and $M = 6$, the FIXED allocation also has a shallower slope in Fig. 4 and the SNR penalties ultimately diverge. However, Fig. 5(b) demonstrates that the SNR penalties for $2 \leq R \leq 14$ are surprisingly small, less than 0.5 and 0.3 dB for $M = 4$ and $M = 6$, respectively. For both the FUSE and FIXED allocations, Fig. 5 confirms that the penalties become small for a moderate M, implying that the convergence of $C_{0,\mathrm{FUSE}}$ and $C_{0,\mathrm{FIXED}}$ toward $C_{0,\mathrm{OPT}}$ is fast.

As observed in Section IV, the SNR penalty is a function of L. When $L = 0$, there is no penalty, while the SNR penalty increases with L. In Fig. 6, we plot the SNR penalty for various L. An interesting observation is that the increasing step size is

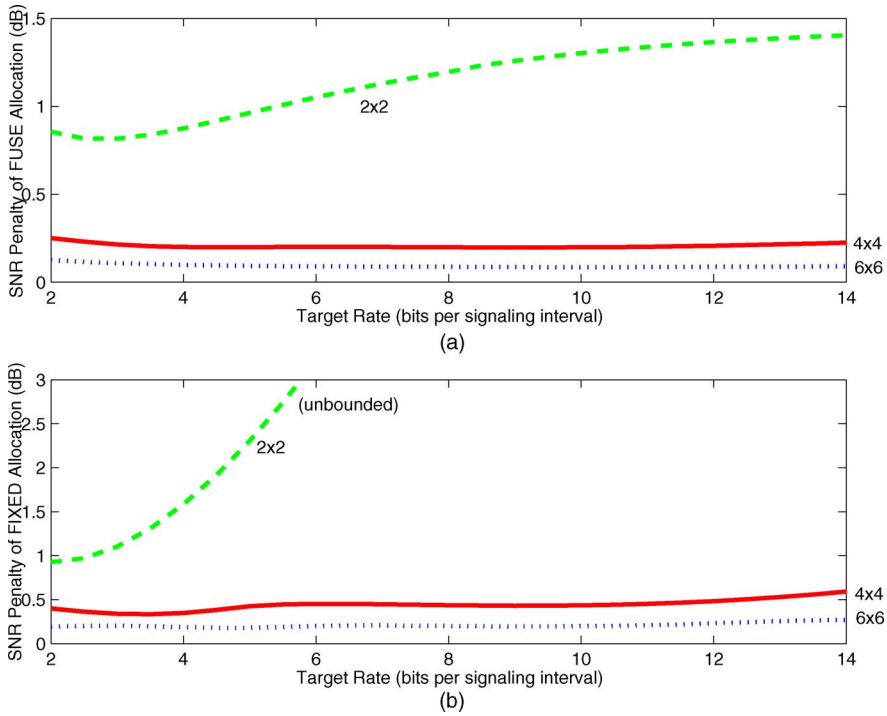

Fig. 5. SNR penalty of the FUSE and FIXED allocations for $M \in \{2, 4, 6\}$ and $L = 4$.

getting smaller as L grows and the SNR penalty looks to converge to a finite value. This agrees with Proposition 5, where we have shown the SNR penalty is finite.

B. Spatially Correlated Channels

In the following, we examine the performance of the FUSE and FIXED allocations when the fading on the transmitter side is spatially uncorrelated, while spatial fading at receive antennas is correlated [17]. This is a typical setting when the receiver is located in open space so that no local scattering occurs around receive antennas. Let $\mathbf{R}_l = \mathbb{E}[\boldsymbol{g}_{l,k}\boldsymbol{g}_{l,k}^*]$ be the correlation matrix for the lth tap, where $\boldsymbol{g}_{l,k}$ denotes the k-th column of the matrix $\mathbf{G}_l$. We assume that the fading statistics are the same for all transmit antennas, that is, $\mathbf{R}_l$ is independent of k. Then, each channel matrix is

$$\mathbf{G}_l = (\mathbf{R}_l)^{\frac{1}{2}}\mathbf{Q}_l \tag{36}$$

where $(\mathbf{A})^{\frac{1}{2}}$ denotes the matrix square root, such that $(\mathbf{A})^{\frac{1}{2}}(\mathbf{A})^{\frac{1}{2}} = \mathbf{A}$, and where $\mathbf{Q}_l$ is an $M_R \times M_T$ matrix with independent $\mathcal{CN}(0,1)$ entries. From channel normalization, $\sum_{l=0}^{L} \mathrm{tr}\{\mathbf{R}_l\} = M_R$, where $\mathrm{tr}\{\cdot\}$ denotes the trace of diagonal elements of a square matrix [19]. If the fading is spatially uncorrelated, the correlation matrix reduces to $\mathbf{R}_l = \sigma_l^2 \mathbf{I}_{M_R}$.

When the channel is spatially correlated, the spatial multiplexing gain, defined as $C_0/\log(\bar{E}/N_0)$, is proportional to the rank of $\sum_{l=0}^{L} \mathbf{R}_l$ rather than $M = \min(M_T, M_R)$. As the rank is a function of L, there can be a significant growth in capacity [12], [17].

We use the approximation in [28] for the correlation matrices, such that

$$[\mathbf{R}_l]_{p,q} \approx \sigma_l^2 e^{-j2\pi|p-q|\Delta\cos(\bar{\theta}_l)} e^{-0.5(2\pi|p-q|\Delta\sin(\bar{\theta}_l)\sigma_{\theta_l})^2} \tag{37}$$

where Δ is the antenna spacing relative to wavelength. The two parameters, $\bar{\theta}_l$ and $\sigma_{\theta_l}^2$, denote the average arrival angle and the variance of the angle spread for the lth path, respectively, both in radian. The angle spread indicates the degree of correlation. When $\sigma_{\theta_l} = 0$, the fading at the lth path is totally correlated and each $\mathbf{R}_l$ collapses to a rank-1 matrix.

Based on the correlation model in (36) and (37), we calculate $C_{0,\mathrm{OPT}}$, $C_{0,\mathrm{FUSE}}$, and $C_{0,\mathrm{FIXED}}$ via Monte Carlo simulations. As the rank of $\mathbf{R}_l$ is increasing with L, $C_{0,\mathrm{OPT}}$ also increases notably. Simulations show that this is true for $C_{0,\mathrm{FUSE}}$ and $C_{0,\mathrm{FIXED}}$. Fig. 7 illustrates the SNR penalty of the FUSE allocation for $M = 4$ when the angle spread is either large ($\sigma_{\theta_l} = 0.25$) or small ($\sigma_{\theta_l} = 0$). The SNR penalty of uncorrelated fading is also plotted as a benchmark. We assume that there are $L = 4$ paths, whose average angles $\{\bar{\theta}_l\}$ are $\{0, \pi/3, 2\pi/3, \pi/2\}$. From Fig. 7, it can be seen that the SNR penalties are 0.1 dB for small spread and 0.15 dB for large spread, both of which are less than that of the uncorrelated channel for both small and large spreads. Fig. 7 shows a tendency that the SNR penalty of a spatially correlated channel increases as the angle spread gets larger and in the end will reach the SNR penalty of a spatially uncorrelated channel.

VI. Conclusion

We proposed the FUSE and FIXED allocation strategies for a closed-loop MIMO-OFDM system, as a replacement for the high-complexity optimal solution based on a joint water-filling

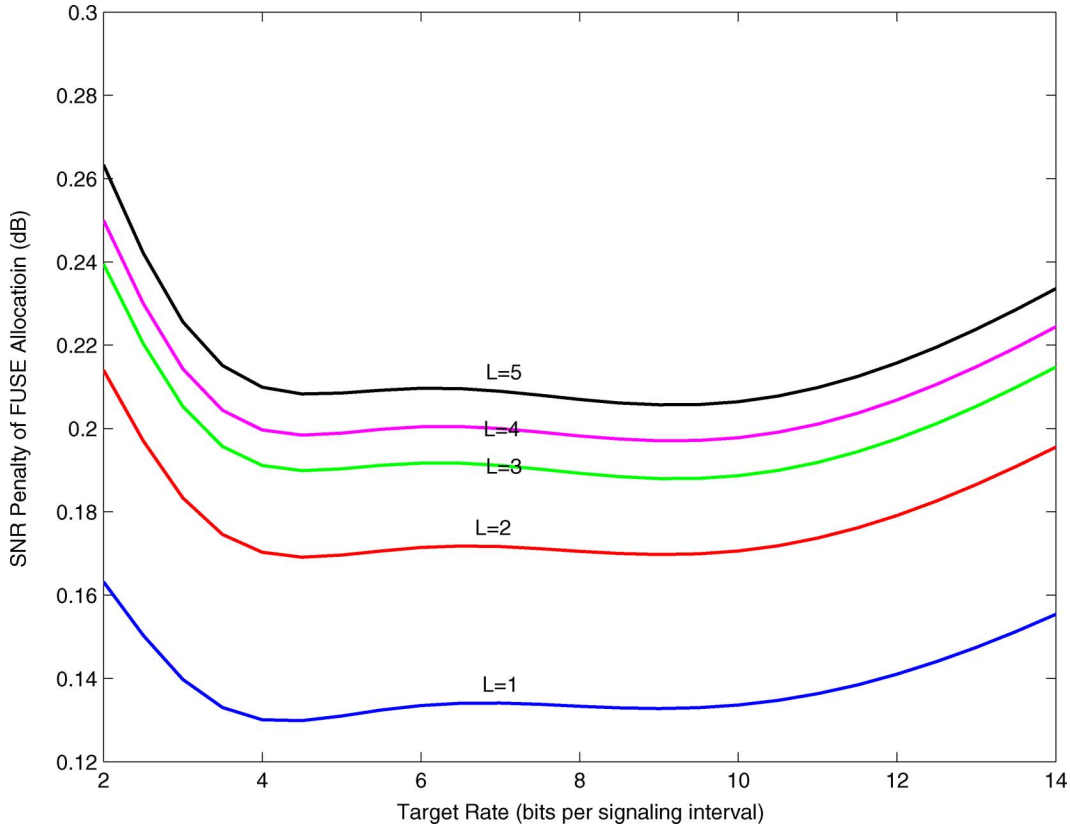

Fig. 6. SNR penalty of the FUSE allocation for $M = 4$ as L grows from 1 to 5.

over space and frequency [8]. We proved that the FUSE and FIXED allocations incur no capacity penalty as the number of antennas tends to infinity. Both strategies are also nearly optimal with a finite number of antennas and high SNR. For example, on a 4×4 Rayleigh channel with memory $L = 4$, the SNR penalty of both FUSE and FIXED allocations is less than 0.5 dB at transmission rates ranging from 2 to 14 bits per signaling interval. This paper theoretically shows that a nonadaptive rate allocation, such as the FIXED allocation, is sufficient to approach the capacity with MIMO-OFDM. Adaptive eigenbeamforming is necessary, but adaptive allocation is not. These theoretical results have important practical implications, since the FUSE and FIXED allocations are readily adapted to give simple and realistic allocation algorithms [14], [15].

Appendix A
Proof of Proposition 5

In this section, we prove Proposition 5. The upper bound in (28) comes from $A_{\mathcal{N}_u} \geq G_{\mathcal{N}_u}$. First, we prove the evaluation of $\mathbb{E}[1/A_{\mathcal{N}_u}]$ in (29) with the uniform power profile. Then, we show the uniform power profile maximizes the upper bound.

Lemma 1:

$$A_{\mathcal{N}_u} = \frac{1}{M} \sum_{l=0}^{L} ||\mathbf{G}_l||_F^2 \tag{38}$$

where $\mathcal{N}_u$ is the universe index set in (6), and $||\mathbf{A}||_F$ denotes the Frobenius norm of a matrix $\mathbf{A}$ [19].

Proof: From the definition of arithmetic mean

$$A_{\mathcal{N}_u} = \frac{1}{MN} \sum_{n=1}^{N} \sum_{m=1}^{M} s_n^{(m)} = \frac{1}{MN} \sum_{n=1}^{N} ||\mathbf{H}_n||_F^2. \tag{39}$$

Since $||\mathbf{H}_n||_F^2 = \sum_{p=1}^{M_R} \sum_{q=1}^{M_T} \left|[\mathbf{H}_n]_{p,q}\right|^2$, we have

$$\begin{aligned}\sum_{n=1}^{N} ||\mathbf{H}_n||_F^2 &= \sum_{n=1}^{N} \sum_{p=1}^{M_R} \sum_{q=1}^{M_T} |[\mathbf{H}_n]_{p,q}|^2 \\ &= \sum_{p=1}^{M_R} \sum_{q=1}^{M_T} \sum_{n=1}^{N} \left| \sum_{l=0}^{L} [\mathbf{G}_l]_{p,q} e^{j2\pi ln/N} \right|^2 \\ &= \sum_{p=1}^{M_R} \sum_{q=1}^{M_T} \sum_{n=1}^{N} \left\{ \sum_{l=0}^{L} |[\mathbf{G}_l]_{p,q}|^2 \right. \\ &\quad \left. + \sum_{l \neq l'} 2\mathrm{Re}\left[[\mathbf{G}_l]_{p,q} [\mathbf{G}_l]_{p,q}^* e^{-j2\pi(l-l')n/N} \right] \right\}. \end{aligned} \tag{40}$$

Since $\sum_{n=1}^{N} e^{-j2\pi(l-l')n/N} = 0$, (40) reduces to

$$\sum_{n=1}^{N} ||\mathbf{H}_n||_F^2 = \sum_{l=0}^{L} \sum_{p=1}^{M_R} \sum_{q=1}^{M_T} \sum_{n=1}^{N} |[\mathbf{G}_l]_{p,q}|^2 = N \sum_{l=0}^{L} ||\mathbf{G}_l||_F^2. \tag{41}$$

Substituting (41) into (39), we obtain (38). □

With the uniform power profile, (38) becomes

$$A_{\mathcal{N}_u} = \frac{1}{M} \sum_{l=0}^{L} ||\mathbf{G}_l||_F^2 = \frac{1}{M(L+1)} \sum_{l=0}^{L} ||\mathbf{Q}_l||_F^2 \tag{42}$$

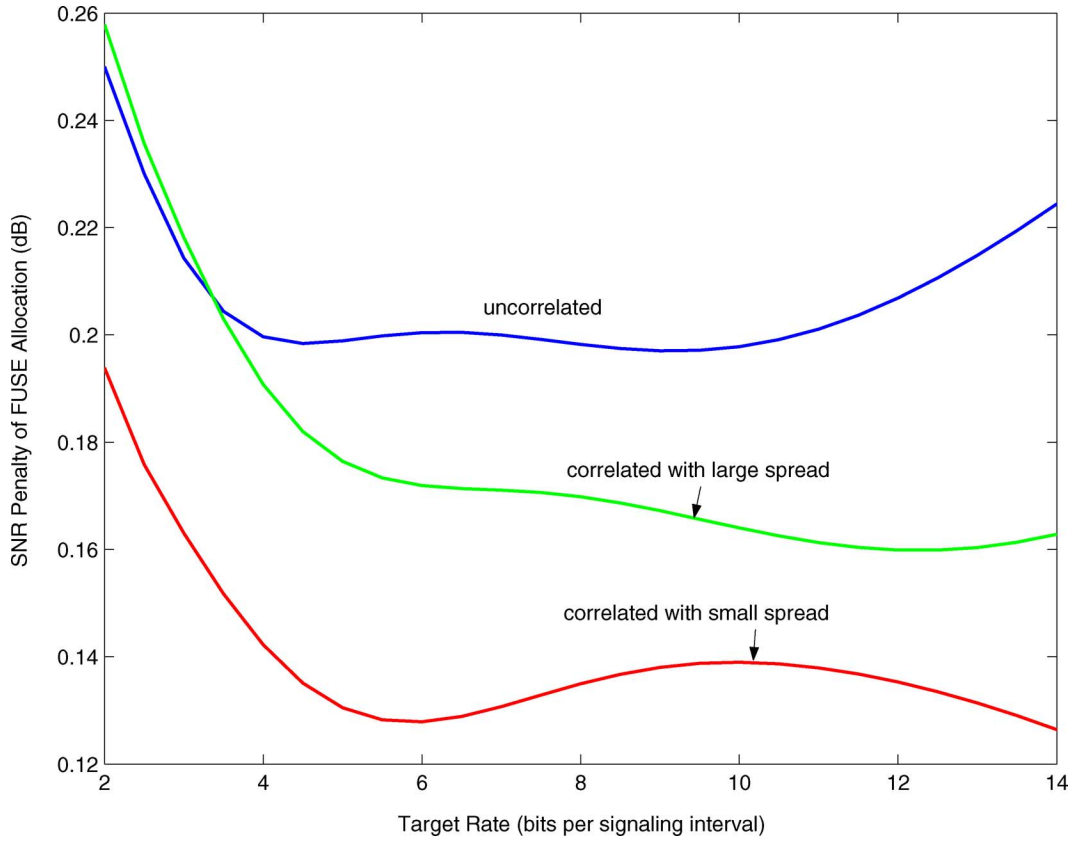

Fig. 7. SNR penalty of the FUSE allocation when spatially correlated for both the large spread ($\sigma_{\theta_l} = 0.25$) and small spread ($\sigma_{\theta_l} = 0$) when $L = 4$ and $M = 4$.

where the elements of $\mathbf{Q}_l$ are i.i.d. $\mathcal{CN}(0,1)$. Then, $M(L+1)A_{\mathcal{N}_u}$ is a chi-square random variable with $M_T M_R(L+1)$ degrees of freedom. We can evaluate $\mathbb{E}[1/A_{\mathcal{N}_u}]$ with the distribution function

$$f_{M(L+1)A_{\mathcal{N}_u}}(x) = \frac{x^{M_T M_R(L+1)-1}e^{-x}}{\Gamma(M_T M_R(L+1))} \quad x \geq 0 \tag{43}$$

where

$$\Gamma(x) = \int_0^\infty t^{x-1}e^{-t}dt \tag{44}$$

is the Gamma function [29]. Then, we have the assertion in (29).

Second, to show that the uniform power profile maximizes the upper bound in (28), we consider the following lemma.

Lemma 2: Suppose that $\boldsymbol{x} = [X_0, X_1, \ldots, X_L]^T$ is an $(L+1) \times 1$ vector, whose elements are i.i.d. random variables with $\Pr[X_l > 0] = 1$. Let $Z = \boldsymbol{s}^T\boldsymbol{x}$ be a scalar, where $\boldsymbol{s} = [\sigma_0^2, \sigma_1^2, \ldots, \sigma_L^2]^T$ is an $(L+1) \times 1$ deterministic vector. Then, $\{\sigma_l^2\}$ that minimize $\mathbb{E}[1/Z]$ subject to $\sum_{l=0}^L \sigma_l^2 = 1$ are

$$\sigma_0^2 = \sigma_1^2 = \cdots = \sigma_L^2 = \frac{1}{L+1}. \tag{45}$$

Proof: Let $f(\boldsymbol{s}) = \mathbb{E}[1/Z]$ be a function from a vector space $\mathcal{S} = \{\boldsymbol{s}; \sum_{l=0}^L \sigma_l^2 = 1\}$ to a real scalar value. For any $\boldsymbol{s}_1$ and $\boldsymbol{s}_2$ belonging to $\mathcal{S}$, we have the inequality:

$$\begin{aligned}\lambda f(\boldsymbol{s}_1) + (1-\lambda) f(\boldsymbol{s}_2) &\overset{(a)}{=} \mathbb{E}\left[\frac{\lambda}{\boldsymbol{s}_1^T\boldsymbol{x}} + \frac{1-\lambda}{\boldsymbol{s}_2^T\boldsymbol{x}}\right] \\ &\overset{(b)}{\geq} \mathbb{E}\left[\frac{1}{\lambda\boldsymbol{s}_1^T\boldsymbol{x} + (1-\lambda)\boldsymbol{s}_2^T\boldsymbol{x}}\right] \\ &= f(\lambda\boldsymbol{s}_1 + (1-\lambda)\boldsymbol{s}_2)\end{aligned} \tag{46}$$

if $0 \leq \lambda \leq 1$, where (a) comes from the fact that $\mathbb{E}[\cdot]$ is a linear operator. The inequality (b) is because $g(x) = x^{-1}(x > 0)$ is convex:

$$\lambda g(\boldsymbol{s}_1^T\boldsymbol{x}) + (1-\lambda) g(\boldsymbol{s}_2^T\boldsymbol{x}) \geq g(\lambda\boldsymbol{s}_1^T\boldsymbol{x} + (1-\lambda)\boldsymbol{s}_2^T\boldsymbol{x}) \tag{47}$$

for $0 \leq \lambda \leq 1$. Therefore, from (46), $f(\boldsymbol{s})$ is convex.

Define an $(L+1) \times (L+1)$ permutation matrix

$$\mathbf{P} = \begin{bmatrix} \mathbf{0}_{L\times 1}^T & 1 \\ \mathbf{I}_L & \mathbf{0}_{L\times 1} \end{bmatrix} \tag{48}$$

where $\mathbf{0}_{L\times 1}$ denotes an $N\times 1$ all-zero vector. Note that $\mathbf{P}^0 = \mathbf{P}^{L+1} = \mathbf{I}_{L+1}$. Then we have

$$f(\boldsymbol{s}) \overset{(a)}{=} \frac{1}{L+1}\sum_{l=0}^{L} f(\mathbf{P}^l\boldsymbol{s}) \overset{(b)}{\geq} f\left(\frac{1}{L+1}\sum_{l=0}^{L}\mathbf{P}^l\boldsymbol{s}\right)$$

where (a) is true because $\{X_l\}$ are i.i.d. and thus the order of $\{\sigma_l^2\}$ does not matter, that is, $f(\boldsymbol{s}) = f(\mathbf{P}^l\boldsymbol{s})$ for any l, and where (b) comes from Jensen's inequality [13] since $f(\boldsymbol{s})$ is convex. The equality in (b) holds if and only if $\{\mathbf{P}^l\boldsymbol{s}\}$ are constant. Therefore, from $\sum_{l=0}^{L}\sigma_l^2 = 1$, we prove that (45) minimizes $\mathbb{E}[1/Z]$. □

From (38), the arithmetic mean is $A_{\mathcal{N}_u} = \sum_{l=0}^{L}\sigma_l^2\|\mathbf{Q}_l\|_F^2$, where the elements of $\mathbf{Q}_l$ are i.i.d. $\mathcal{CN}(0,1)$. Then, by letting $X_l = \|\mathbf{Q}_l\|_F^2/M$, we prove the assertion.

Appendix B
Proof of Proposition 6

The proof is similar to Theorem 2 [8]. Let $g_n^{(m)} = 1/\mathbb{E}[1/s_n^{(m)}]$. First, we derive a lower bound for $C_{0,\mathrm{FIXED}}$, which holds for all SNR. From Proposition 3, we have

$$\rho = \mathbb{E}\left[\sum_{m=1}^{\tilde{M}}\left\{\frac{\nu g_n^{(m)}}{s_n^{(m)}} - \frac{1}{s_n^{(m)}}\right\}^+\right] \leq \mathbb{E}\left[\sum_{m=1}^{\tilde{M}}\frac{\nu g_n^{(m)}}{s_n^{(m)}}\right] = \tilde{M}\nu. \tag{49}$$

Then

$$\begin{aligned} C_{0,\mathrm{FIXED}} &= \sum_{m=1}^{\tilde{M}}\left\{\log_2\left(\nu g_n^{(m)}\right)\right\}^+ \\ &\geq \sum_{m=1}^{\tilde{M}}\log_2\left(\nu g_n^{(m)}\right) \\ &\geq \sum_{m=1}^{\tilde{M}}\log_2\left(\frac{\rho g_n^{(m)}}{\tilde{M}}\right) \end{aligned} \tag{50}$$

where the second inequality comes from (49). Thus, we have the inequality

$$C_{0,\mathrm{FIXED}} \geq M\log_2\left(\frac{\rho}{\tilde{M}}\right) + M\log_2\left(\Gamma_{\tilde{\mathcal{N}}}\right) \tag{51}$$

where $\Gamma_{\tilde{\mathcal{N}}}$ is the geometric mean in (35), which is identical for all n.

On the other hand, we consider a region

$$\left\{\left[g_n^{(1)},\ldots,g_n^{(\tilde{M})}\right]; g_n^{(\tilde{M})} > \Gamma_{\tilde{\mathcal{N}}}2^{-R/\tilde{M}}\right\} \tag{52}$$

for which we use all $\tilde{M}$ channels at a rate of R, such that $|\mathcal{M}_{\mathrm{FIXED}}|$ in Proposition 3 is $\tilde{M}$. Then

$$\begin{aligned} \rho &\geq \mathbb{E}\left[\sum_{m=1}^{\tilde{M}}\frac{2^{R/\tilde{M}}g_n^{(m)}}{\Gamma_{\tilde{\mathcal{N}}}s_n^{(m)}} - \frac{1}{s_n^{(m)}}\right]1\left\{g_n^{(\tilde{M})} > \Gamma_{\tilde{\mathcal{N}}}2^{-R/\tilde{M}}\right\} \\ &= \left(\frac{2^{R/\tilde{M}}}{\Gamma_{\tilde{\mathcal{N}}}} - \mathbb{E}\left[\frac{1}{s_n^{(m)}}\middle| 1\left\{g_n^{(\tilde{M})} > \Gamma_{\tilde{\mathcal{N}}}2^{-R/\tilde{M}}\right\}\right]\right). \end{aligned} \tag{53}$$

As $R\to\infty$

$$\mathbb{E}\left[\frac{1}{s_n^{(m)}}\middle| 1\left\{g_n^{(\tilde{M})} > \Gamma_{\tilde{\mathcal{N}}}2^{-R/\tilde{M}}\right\}\right] \to \mathbb{E}\left[\frac{1}{s_n^{(m)}}\right] < \infty. \tag{54}$$

Therefore, (53) asymptotically becomes

$$C_{0,\mathrm{FIXED}} \leq M\log_2\left(\frac{\rho}{\tilde{M}}\right) + M\log_2\left(\Gamma_{\tilde{\mathcal{N}}}\right) \tag{55}$$

at high SNR. From (51) and (55), we have the assertion in (34).

Acknowledgment

The authors are most grateful to the Associate Editor and the anonymous reviewers, whose constructive comments allowed them to improve the technical quality as well as the legibility of the paper.

References

[1] E. Biglieri, J. Proakis, and S. Shamai (Shitz), "Fading channels: Information-theoretic and communication aspects," *IEEE Trans. Inf. Theory*, vol. 44, pp. 2619–2692, Oct. 1998.
[2] A. J. Goldsmith and P. P. Varaiya, "Capacity of fading channels with channel side information," *IEEE Trans. Inf. Theory*, vol. 43, pp. 1986–1992, Nov. 1997.
[3] C. Chuah, D. Tse, J. Kahn, and R. A. Valenzuela, "Capacity scaling of MIMO wireless systems under correlated fading," *IEEE Trans. Inf. Theory*, vol. 48, pp. 637–650, Mar. 2002.
[4] G. J. Foschini, Jr. and M. J. Gans, "On limits of wireless communication in a fading environment when using multiple antennas," *Wireless Pers. Commun.*, pp. 36–54, Mar. 1998.
[5] I. E. Telatar, "Capacity of multi-antenna Gaussian channels," *European Trans. Telecommun.*, vol. 10, pp. 585–595, Nov./Dec. 1999.
[6] A. Grant, "Rayleigh fading multi-antenna channels," *EURASIP JASP*, vol. 2002, no. 3, pp. 316–329, Mar. 2002.
[7] G. Caire, G. Taricco, and E. Biglieri, "Optimum power control over fading channels," *IEEE Trans. Inf. Theory*, vol. 45, pp. 1468–1489, Jul. 1999.
[8] E. Biglieri, G. Caire, and G. Taricco, "Limiting performance of block-fading channels with multiple antennas," *IEEE Trans. Inf. Theory*, vol. 47, pp. 1273–1289, May 2001.
[9] S. Hanly and D. Tse, "Multi-access fading channels—Part II: Delay-limited capacities," *IEEE Trans. Inf. Theory*, vol. 44, pp. 2816–2831, Nov. 1998.

[10] G. L. Stüber, *Principles of Mobile Communication*. New York: Kluwer Academic, 1996.
[11] M.-S. Alouni and A. J. Goldsmith, "Capacity of Rayleigh fading channels under different adaptive transmission and diversity-combining techniques," *IEEE Trans. Veh. Technol.*, vol. 48, no. 4, pp. 1165–1181, Jul. 1999.
[12] G. G. Raleigh and J. M. Cioffi, "Spatio-temporal coding for wireless communication," *IEEE Trans. Commun.*, vol. 46, pp. 357–366, Mar. 1998.
[13] T. M. Cover and J. A. Thomas, *Elements of Inform. Theory*. New York: Wiley, 1991.
[14] J. H. Sung and J. R. Barry, "Bit-allocation strategies for MIMO fading channels with channel knowledge at transmitter," in *Proc. IEEE Veh. Technol. Conf. (VTC) 2003 Spring*, Jeju, Korea, 2003, pp. 813–817.
[15] J. H. Sung and J. R. Barry, "Rate-allocation strategies for closed-loop MIMO OFDM," in *Proc. IEEE Veh. Technol. Conf. (VTC) 2003 Fall*, Orlando, FL, USA, 2003, pp. 483–487.
[16] J. R. Barry, E. A. Lee, and D. G. Messerschmitt, *Digital Communication*, 3rd ed. New York: Kluwer Academic, 2003.
[17] H. Bölcskei, D. Gesbert, and A. J. Paulraj, "On the capacity of OFDM-based spatial multiplexing systems," *IEEE Trans. Commun.*, vol. 50, pp. 225–234, Feb. 2002.
[18] A. Scaglione and A. Salhotra, "The statistics of the MIMO frequency selective fading AWGN channel capacity," *IEEE Trans. Inf. Theory*, submitted for publication.
[19] R. A. Horn and C. R. Johnson, *Matrix Analysis*. Cambridge, U.K.: Cambridge University Press, 1985.
[20] C. Brunner, W. Utschick, and J. A. Nossek, "Exploiting the short-term and long-term channel properties in space and time: Eigenbeamforming concepts for the BS in WCDMA," *European Trans. Telecommun.*, vol. 12, no. 5, pp. 365–378, 2001.
[21] T. P. Kurpjuhn, M. Joham, W. Utschick, and J. A. Nossek, "Experimental studies about eigenbeamforming in standardization MIMO channels," in *Proc. IEEE Veh. Technol. Conf. (VTC) 2002 Fall*, Vancouver, Canada, 2002, pp. 185–189.
[22] R. A. Berry and R. G. Gallager, "Communication over fading channels with delay constraint," *IEEE Trans. Inf. Theory*, vol. 48, pp. 1135–1149, May 2002.
[23] R. R. Müller, "A random matrix model of communication via antenna arrays," *IEEE Trans. Inf. Theory*, vol. 48, pp. 2495–2506, Sep. 2002.
[24] B. Varadarajan and J. R. Barry, "Optimization of full-rate full-diveristy linear space-time codes using the union bound," in *Proc. 2003 Inf. Theory Workshop*, Paris, France, 2003, pp. 210–213.
[25] L. Zheng and D. Tse, "Diversity and multiplexing: A fundamental tradeoff in multiple antenna channels," *IEEE Trans. Inf. Theory*, vol. 49, pp. 1073–1096, May 2003.
[26] A. Edelman, "Eigenvalues and Condition Numbers of Random Matrices," Ph.D. dissertation, Massachusetts Institute of Technology, Cambridge, MA, 1989.
[27] M. Wennström, "On MIMO Systems and Adaptive Arrays for Wireless Communication: Analysis and Practical Issues," Ph.D., Uppsala University, Uppsala, Sweden, 2002.
[28] D. Asztély, On Antenna Arrays in Mobile Communication Systems: Fast Fading and GSM Base Station Receiver Algorithms Royal Institute of Technology, Stockholm, Sweden, IR-S3-SB-9611, 1996.
[29] I. S. Gradshteyn and I. M. Ryzhik, *Table of Integrals, Series, and Products*, 6th ed. New York: Academic, 2000.